Tomosyn-dependent regulation of synaptic transmission is required for a late phase of associative odor memory

Kaiyun Chen[a,1], Antje Richlitzki[b,1], David E. Featherstone[a,2], Martin Schwärzel[b,2,3], and Janet E. Richmond[a,2,3]

[a]Department of Biological Sciences, University of Illinois at Chicago, Chicago, IL 60607; and [b]Institute for Biology/Genetics, Free University Berlin, D-14195 Berlin, Germany

Edited by Barry Ganetzky, University of Wisconsin, Madison, WI, and approved October 6, 2011 (received for review June 23, 2011)

Synaptic vesicle secretion requires the assembly of fusogenic SNARE complexes. Consequently proteins that regulate SNARE complex formation can significantly impact synaptic strength. The SNARE binding protein tomosyn has been shown to potently inhibit exocytosis by sequestering SNARE proteins in nonfusogenic complexes. The tomosyn–SNARE interaction is regulated by protein kinase A (PKA), an enzyme implicated in learning and memory, suggesting tomosyn could be an important effector in PKA-dependent synaptic plasticity. We tested this hypothesis in *Drosophila*, in which the role of the PKA pathway in associative learning has been well established. We first determined that panneuronal tomosyn knockdown by RNAi enhanced synaptic strength at the *Drosophila* larval neuromuscular junction, by increasing the evoked response duration. We next assayed memory performance 3 min (early memory) and 3 h (late memory) after aversive olfactory learning. Whereas early memory was unaffected by tomosyn knockdown, late memory was reduced by 50%. Late memory is a composite of stable and labile components. Further analysis determined that tomosyn was specifically required for the anesthesia-sensitive, labile component, previously shown to require cAMP signaling via PKA in mushroom bodies. Together these data indicate that tomosyn has a conserved role in the regulation of synaptic transmission and provide behavioral evidence that tomosyn is involved in a specific component of late associative memory.

Synaptic transmission is dependent on the formation of SNARE complexes between the vesicle SNARE synaptobrevin and the plasma membrane SNAREs syntaxin and SNAP-25 (1). SNARE complex assembly produces fusion-competent (primed) vesicles, docked at the plasma membrane (2, 3). Originally identified as a syntaxin-binding protein, tomosyn has emerged as a negative regulator of secretion by directly competing with synaptobrevin to form nonfusogenic tomosyn SNARE complexes (4–6). The N terminus of tomosyn also promotes SNARE complex oligomerization, sequestering SNARE monomers required for priming (7), and impedes the function of the calcium-sensor synaptotagmin (8). By these means tomosyn is involved in regulating SNARE complex assembly and controlling the size of the readily releasable pool of synaptic vesicles. Evidence suggests that the interaction between tomosyn and the SNARE machinery can be modulated by cAMP-dependent protein kinase A (PKA) phosphorylation of tomosyn, a second messenger cascade previously implicated in several forms of behavioral and synaptic plasticity (7, 9–15). Here, we characterized the synaptic function of *Drosophila* tomosyn and probed the functional relevance of tomosyn in the regulation of behavioral plasticity.

Results

RNAi Interference Allows for Targeted Knockdown of Tomosyn. The *Drosophila* genome encodes a single *tomosyn* gene that exhibits 35% amino acid identity to *Caenorhabditis elegans tom-1* and 41% identity to rat tomosyn-m (Fig. 1*A*). Because there are no *Drosophila tomosyn* mutants, to assess the role of tomosyn in *Drosophila* we obtained two fly lines from the Vienna *Drosophila* RNAi Center (http://stockcenter.vdrc.at) carrying the same upstream activation sequence (UAS)-*tomosyn* RNAi transgene on either the second (line II) or third (line III) chromosome. The *tomosyn* RNAi construct targeted the last exon of *tomosyn*, common to all predicted isoforms (Fig. 1*A*). To knockdown tomosyn in neurons, both UAS-*tomosyn* lines were crossed to the panneuronal driver ElavGal4. The extent of RNAi interference was then assessed by quantitative RT-PCR. Both lines exhibited a marked reduction in mRNA levels (an 80% reduction in line II and 65% in line III; Fig. 1*B*). To confirm that loss of transcript reduced tomosyn protein levels, we generated an antibody against *Drosophila* tomosyn. In wild-type third-instar larvae, antitomosyn labeling was highly enriched at neuromuscular junctions (NMJs) but reduced by 70% in line II and 56% in line III (Fig. 1 *C* and *D*), corresponding closely to the drop in mRNA levels. These immunohistochemical data also demonstrate that the tomosyn antibody is specific for fly tomosyn and that tomosyn is primarily expressed presynaptically at the fly NMJ, because the RNAi was restricted to neurons.

Tomosyn Regulates Synaptic Transmission at the NMJ. We next recorded evoked excitatory junctional currents (EJCs) from third-instar larvae NMJs (Fig. 2*A*). The total charge transfer of EJCs was increased by 142% in line II and 130% in line III, compared with controls (Fig. 2*B*). The enhanced EJC charge transfer primarily reflected increased EJC decay time in both RNAi lines (Fig. 2*C*), because marginal increases in EJC amplitude only reached significance for line III (Fig. 2*D*), and neither line exhibited changes in EJC rise time (Fig. 2*E*). To explore the basis for this prolonged release, we examined endogenous miniature synaptic events (mEJCs). There was no difference in mEJC frequency (Fig. 3 *A* and *B*), but mEJCs exhibited an increased decay time (Fig. 3*C*), although this did not result in a significant increase in mEJC charge integral (Fig. 3*D*), despite normal rise times (Fig. 3*E*) and amplitudes (Fig. 3*F*). Dividing the average EJC charge integral by the average mEJC charge integral to determine quantal content indicated that the number of quanta per EJC increased by 119% for RNAi line II and 114% for RNAi line III (Fig. 3*G*). These data suggest that enhanced EJC charge transfer after tomosyn knockdown primarily reflects an increase in the number of vesicles released late in the evoked response.

Measurement of paired-pulse depression (PPD) is thought to be a more sensitive indicator of changes in release levels. Exam-

Author contributions: K.C. and A.R. performed research; K.C., A.R., D.E.F., and J.E.R. analyzed data; D.E.F., M.S., and J.E.R. designed research; and D.E.F., M.S., and J.E.R. wrote the paper.

The authors declare no conflict of interest.

This article is a PNAS Direct Submission.

[1]K.C. and A.R. contributed equally to this work.

[2]To whom correspondence may be addressed. E-mail: def@uic.edu, martin.schwaerzel@fu-berlin.de, or jer@uic.edu.

[3]M.S. and J.E.R. contributed equally to this work.

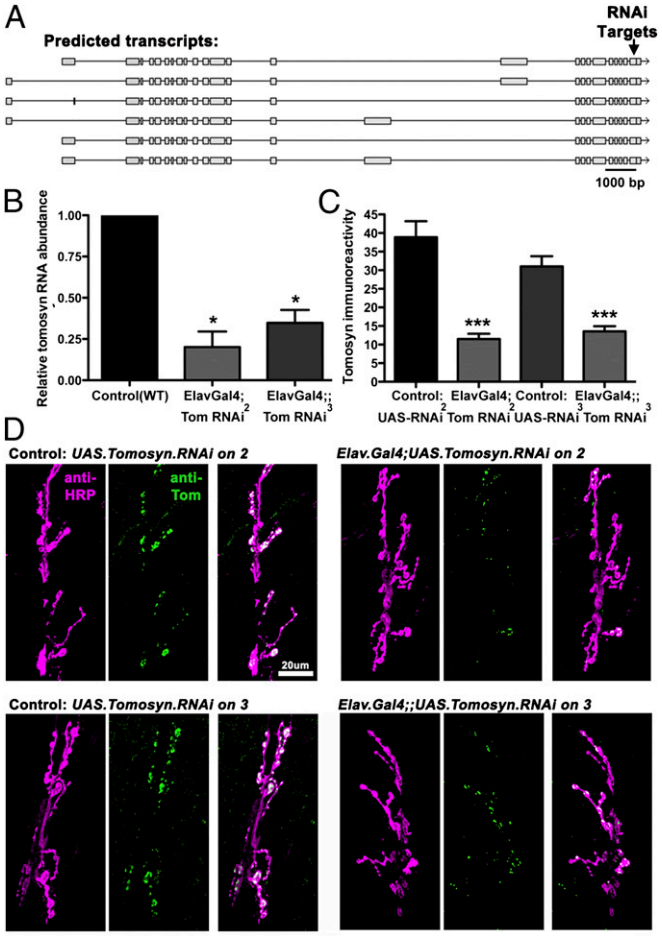

Fig. 1. Knockdown of tomosyn by panneuronal RNAi. (*A*) The *Drosophila tomosyn* gene encodes several predicted transcripts, all of which are targeted by the *tomosyn* RNAi transgene (arrow). (*B* and *C*) Panneuronal expression of *tomosyn* RNAi lines (II and III) using ElavGal4 caused significant loss of total tomosyn RNA, measured using quantitative RT-PCR (*B*), and significant loss of tomosyn immunoreactivity at larval neuromuscular junctions (*C*). (*D*) Representative confocal images of larval NMJs stained with anti-HRP antibodies to visualize neuronal membrane (magenta) and anti-tomosyn antibodies to visualize tomosyn protein (green).

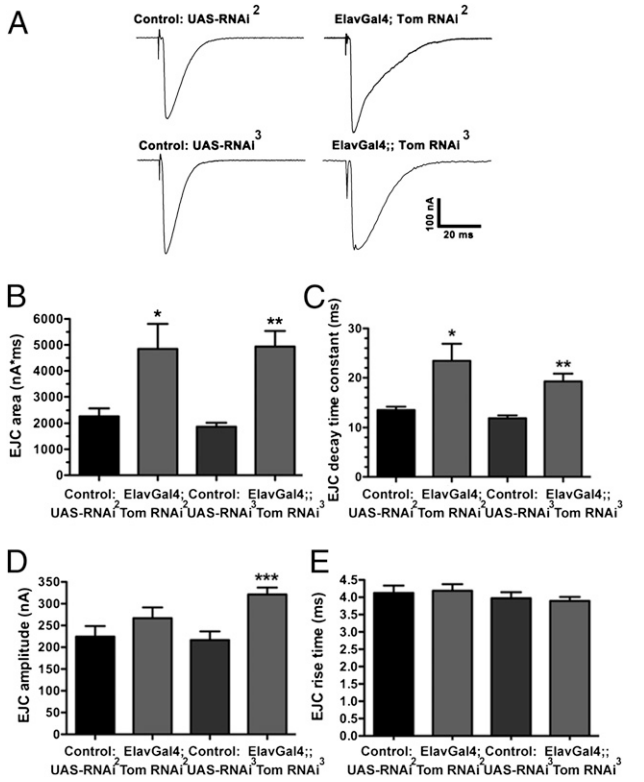

Fig. 2. *Tomosyn* RNAi enhances release at the NMJ. (*A*) Representative EJCs of larval NMJs. (*B*) EJC area (nA*ms) is significantly increased by panneuronal expression of *tomosyn* RNAi, compared with controls carrying the unexpressed RNAi transgene(s). (*C*) EJC decay time constants are significantly increased by neuronal expression of *tomosyn* RNAi. (*D*) EJC amplitude is slightly but not consistently increased by expression of *tomosyn* RNAi. (*E*) EJC rise time is not changed by panneuronal expression of *tomosyn* RNAi.

ination of PPD at the NMJ after *tomosyn* RNAi also showed a significant increase for both line II (20% increase) and line III (22% increase), consistent with the hypothesis that tomosyn knockdown enhances release, possibly resulting in depletion of the readily releasable pool during the first evoked response (Fig. 4 *A* and *B*).

In cultured vertebrate neurons, tomosyn knockdown affects both neurite outgrowth and synaptic coupling (9). To determine whether the changes in EJCs after *tomosyn* RNAi at fly NMJs reflect alterations in synaptogenesis, bouton density (Fig. 5*B*) and area (Fig. 5*C*) of HRP-labeled motorneurons (Fig. 5*A*) was measured. Neither *tomosyn* RNAi line significantly changed these parameters. Together these data indicate that the enhanced release at the NMJ after tomosyn knockdown is due to changes in exocytic function rather than altered synaptic architecture.

PKA phosphorylation of tomosyn has been shown to reduce its syntaxin binding affinity, thereby regulating the inhibitory action of tomosyn in cultured neurons (10). To examine whether the cAMP pathway potentially regulates tomosyn function at *Drosophila* synapses, we examined the effects of cAMP activation on NMJ EJC kinetics. Perfusion of the adenylate-cyclase activator forskolin produced a significant increase in EJC charge transfer, similar to the effects of *tomosyn* RNAi (Fig. 6*A*). To test whether tomosyn and cAMP act in the same pathway, we next examined the effects of forskolin on NMJs after *tomosyn* RNAi. The enhanced EJC charge integral resulting from *tomosyn* knockdown was not further increased upon forskolin application (Fig. 6*B*). These data suggest that tomosyn may be an important downstream target of cAMP signaling at fly synapses.

Tomosyn Differentiates Between Early and Late Aversive Odor Memory. To probe the functional relevance of tomosyn in behavioral plasticity, we assayed early (3 min; Fig. 7*A*) and late (3 h; Fig. 7*B*) memory performance after aversive olfactory conditioning. Early memory was indistinguishable between RNAi-treated and control animals bearing either the ElavGal4 element or UAS-*tomosyn* elements alone. In contrast, late memory was reduced by ≈50% after tomosyn knockdown. Thus, panneuronal *tomosyn* RNAi differentiates between early and late aversive odor memory.

Late memory is a composite of two components: a stable component operationally defined on the basis of resistance to cold anesthesia [anesthesia-resistant memory (ARM)], and a labile component that is abolished by cold anesthesia [anesthesia-sensitive memory (ASM)] (14, 16, 17). To test whether tomosyn is preferentially involved in either memory component, we applied cold anesthetic treatment 30 min before measuring late memory performance, thus selectively measuring the ARM component of late memory. The ASM component of late memory is reflected by the difference between composite late memory (measured without cooling) and ARM (measured with cooling; Fig. 8*A*). This analysis revealed a specific effect of tomosyn knockdown on ASM, whereas ARM remained indistinguishable from wild-type levels.

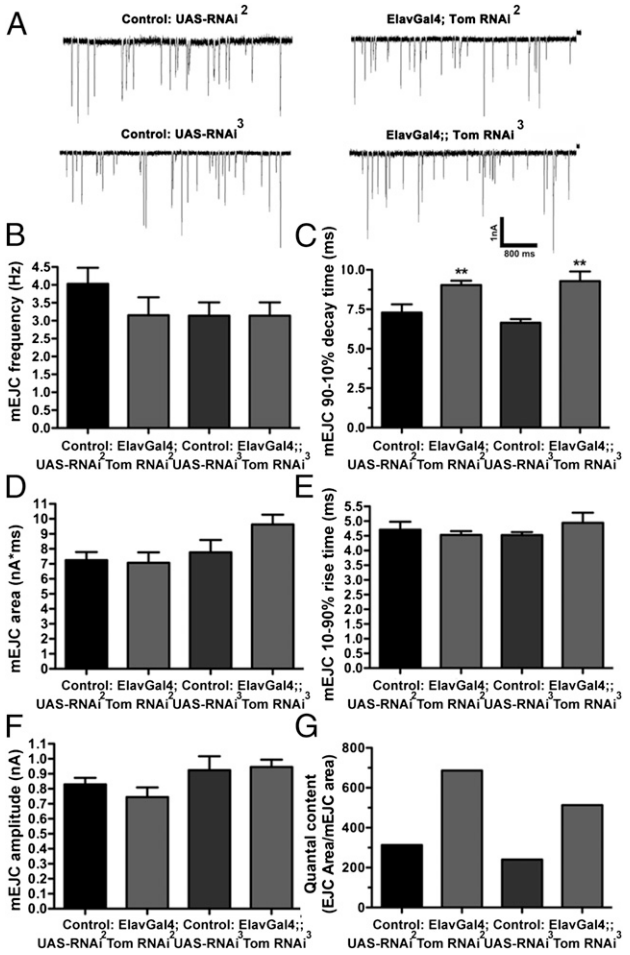

Fig. 3. *Tomosyn* RNAi enhances mEJC duration and quantal content. (*A*) Representative mEJCs recorded from larval NMJs after panneuronal expression of *tomosyn* RNAi and controls carrying the unexpressed RNAi transgene. (*B*) mEJC frequency is not significantly altered by expression of *tomosyn* RNAi. (*C*) mEJC decay time constants are significantly increased after *tomosyn* RNAi. (*D–F*) *Tomosyn* RNAi does not significantly increase mEJC area (*D*), rise time (*E*), or amplitude (*F*). (*G*) Because of the increase in EJC area (Fig. 2), quantal content is increased after expression of *tomosyn* RNAi.

Late-Phase ASM Requires Tomosyn Within the Major Intrinsic Neurons of the Mushroom Bodies. The *Drosophila* olfactory pathway follows a stereotyped organization orthologous to the mammalian olfactory bulb (18): airborne chemicals activate olfactory receptor neurons (ORNs), which project to the antennal lobes, where information is computed by local neurons (LNs) and projection neurons (PNs) and conveyed to the lateral protocerebrum and mushroom bodies (19–21). To probe which layers of this circuitry require tomosyn function to support late-phase ASM, we used Gal4 lines driving expression of UAS-*tomosyn* RNAi in either ORNs, LNs, PNs, or mushroom bodies. *Tomosyn* RNAi only reduced late odor memory performance when targeted to mushroom body intrinsic neurons (Fig. 8*B*), although we cannot completely exclude the possible contribution of other brain areas affected by the Gal4 (Ok107) driver used for this experiment. As expected, this reduction in late memory performance in mushroom bodies was due to specific loss of late ASM, as revealed by application of cold anesthesia before memory recall.

Discussion

Our results demonstrate that tomosyn suppresses synaptic function and is necessary in mushroom body intrinsic neurons

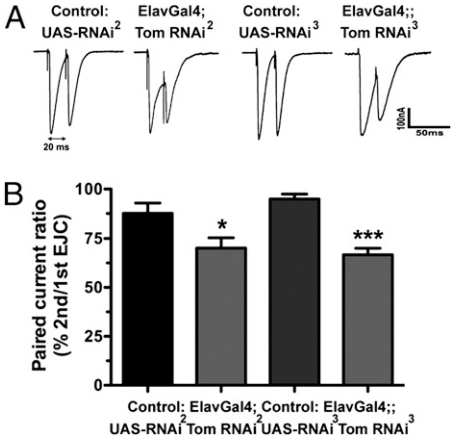

Fig. 4. PPD is enhanced after *tomosyn* RNAi. (*A*) Representative EJC pairs with a 20-ms interval. (*B*) Although the amplitude of the second EJC is normally reduced compared with the first EJC, the reduction is significantly larger after expression of *tomosyn* RNAi.

specifically for a long-term cAMP-dependent component of associative olfactory learning in *Drosophila*.

Tomosyn Suppresses Synaptic Function. The prominent biophysical change observed at the fly NMJ after *tomosyn* RNAi is a prolonged EJC resulting in an increased total charge transfer, similar to that observed at *C. elegans tomosyn* mutant synapses (22, 23). Although the underlying cause of the altered EJC duration in either *C. elegans* or *Drosophila* has yet to be determined, one potential explanation is the occurrence of late fusion events possibly resulting from ectopically primed vesicles distal to release sites. This hypothesis is supported by ultrastructural data from *C. elegans tomosyn* mutants, in which a twofold increase in the number of morphologically docked vesicles was observed, the additional vesicles positioned further from the presynaptic density (22). Analyses of priming defective *unc-13* and *syntaxin C. elegans* mutants, in which docked vesicles were found to be greatly reduced, suggest that vesicle docking is a morphological correlate of priming (3, 24, 25). On the basis of these data, it has been proposed that distally primed vesicles in *C. elegans tomosyn* mutants

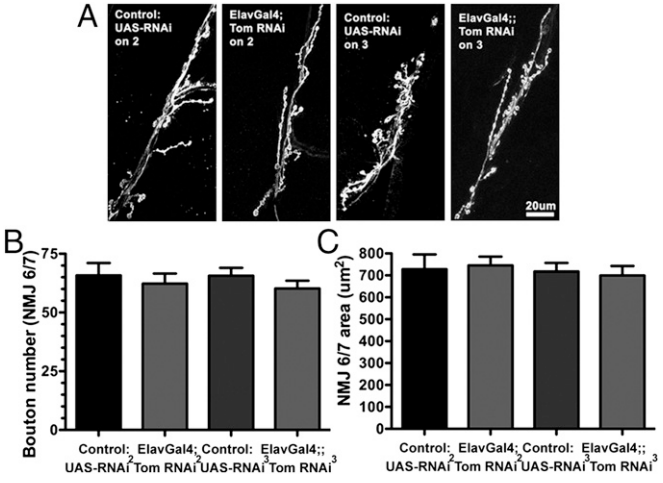

Fig. 5. Synaptic morphology is unaffected by tomosyn knockdown. (*A*) Representative confocal images of muscles 6 and 7 NMJs stained with anti-HRP antibodies to visualize presynaptic morphology. (*B* and *C*) Panneuronal expression of *tomosyn* RNAi does not affect the number of presynaptic boutons (*B*) or NMJ size (*C*).

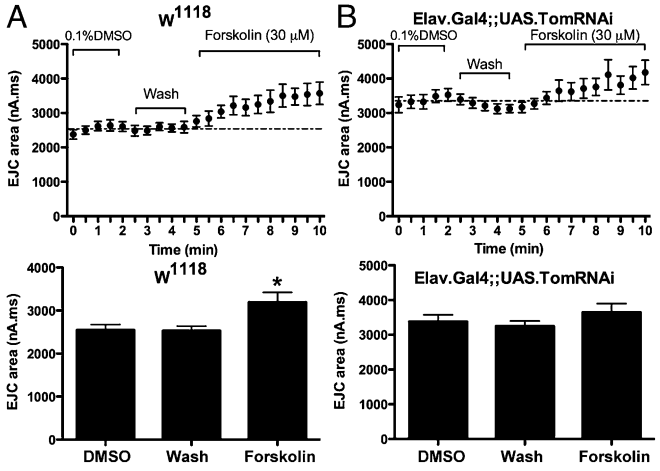

Fig. 6. *Tomosyn* RNAi occludes cAMP-dependent synaptic enhancement. (*A*) Bath application of 30 uM forskolin in DMSO increases EJC charge integral at the NMJ. (*B*) Forskolin application does not further enhance EJC charge integral in larvae expressing panneuronal *tomosyn* RNAi.

exhibit delayed release relative to those close to the presynaptic density, the presumed site of calcium entry, leading to a broadened evoked response (22).

The observed increase in synaptic release at the fly NMJ after *tomosyn* RNAi adds to a growing body of evidence that tomosyn suppresses synaptic strength. For example, the twofold increase in docked vesicles observed at *C. elegans tomosyn* mutant synapses correlates with a doubling of the readily releasable pool assessed by applying hyperosmotic saline and corresponds to the enhanced evoked EJC charge integral (22). The increase in quantal content and reduction in PPD at the fly NMJ after *tomosyn* RNAi is also consistent with an enhanced primed vesicle pool. Similar conclusions were reached for changes in paired-pulse facilitation at central synapses of mouse *tomosyn* mutants (7).

The observation that tomosyn knockdown at the fly NMJ results in the addition of mEJCs with slower decay kinetics could also be a manifestation of ectopic vesicle priming. Alternatively, this change in fly mEJCs could reflect a change in fusion pore dynamics in the absence of tomosyn, a possibility given previously observed genetic and/or physical interactions between tomosyn and several key components of the exocytic machinery, including the SNARE proteins synaptotagmin, Munc-13, and Munc-18 (4, 8, 22, 23, 26). Because the presynaptic density is responsible for localizing elements of the vesicle fusion machinery such as UNC-13 and calcium channels (24, 27), spatial misregulation of vesicle docking in the absence of tomosyn may be related to these changes in fusion properties. However, definitive evidence for ectopically primed vesicles at the fly NMJ after *tomosyn* RNAi is not yet available, and therefore the cause of the altered evoked response kinetics remains speculative.

Evidence indicates that vertebrate tomosyn is a PKA target (10). Although we cannot yet definitively establish that tomosyn function is down-regulated by PKA phosphorylation at fly synapses pending the availability of a *tomosyn* null mutant, the fact that *tomosyn* RNAi phenocopies the NMJ response to cAMP activa-

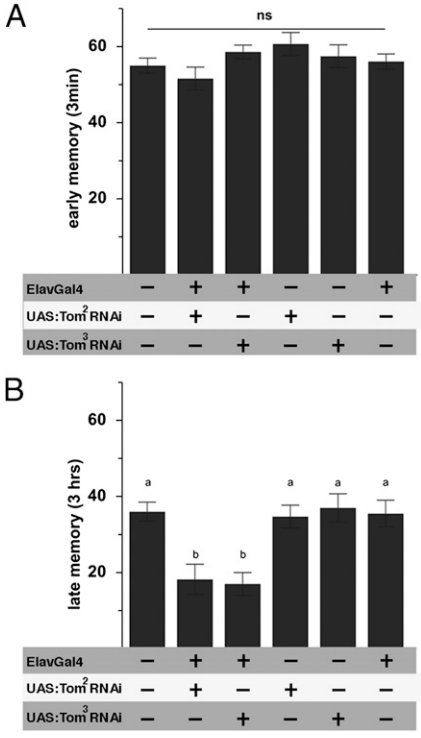

Fig. 7. Tomosyn dissociates between early and late associative odor memories. (*A*) Aversive associative memory performance in adult *Drosophila* 3 min after training (early memory) was independent of tomosyn function, whereas 3-h (late) memory was severely reduced (*B*) in flies expressing *tom*-specific RNAi throughout the CNS. Genetic controls bearing either ElavGal4 or appropriate RNAi constructs alone performed at a level indistinguishable from wild type. All data represent means ± SEM; $n \geq 7$. Different characters indicate statistical differences at a level of $P \leq 0.01$; ns, no difference at a level of $P \geq 0.05$.

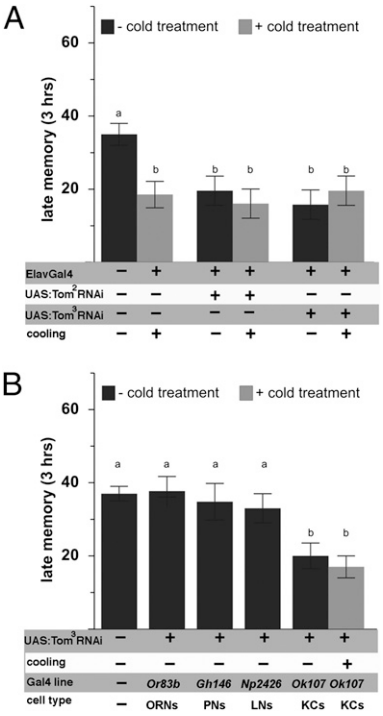

Fig. 8. Tomosyn supports late ASM. The ASM and ARM components of late memory were dissociated by application of cold anesthetic treatment before recall (black and gray bars). (*A*) Panneuronal knockdown of tomosyn did not interfere with ARM performance but completely abolished ASM. (*B*) Tissue-specific knockdown of tomosyn within the olfactory circuitry identified mushroom body Kenyon cells as necessary for tomosyn function in ASM. All data represent means ± SEM; $n \geq 6$. KCs, Kenyon cells. Different characters indicate statistical differences at a level of $P \leq 0.01$; ns, no difference at a level of $P \geq 0.05$.

tion and that these two treatments show nonadditivity supports this notion.

On the basis of our analysis of NMJ function, we predict that, as in mouse *tomosyn* mutants, synapses within the fly CNS will experience similar increases in synaptic strength after *tomosyn* RNAi or cAMP activation. This prediction is supported by the specific ASM aversive odor learning deficit observed in the fly olfactory CNS after tomosyn knockdown in mushroom body Kenyon cells, the site of cAMP-mediated associative memory formation.

Tomosyn Is Required for cAMP-Dependent Associative Learning. *Drosophila* aversive odor learning has long been used to investigate the molecular and cellular mechanisms underlying associative memory formation (28–32). In the *Drosophila* mushroom bodies, neuronal signals representing odor cues and electric shock converge onto type I adenylyl cyclase encoded by *rutabaga (rut-AC I)* to initiate cAMP signals necessary and sufficient to form engrams underlying associative odor memory. These instructive cAMP signals localize to the Kenyon cells in which presynaptic changes are thought to represent a particular odor memory (33–35). Stabilization of aversive odor memory over time requires signals from dorsal-paired medial (DPM) neurons, the putative release sites of amnesiac peptide—the fly homolog to mammalian pituitary adenylate cyclase-activating polypeptide (PACAP) (36, 37)—onto mushroom body Kenyon cells. Amnesiac neuropeptides are known to stimulate cAMP production (38, 39), whereas the major fly PKA is required from 30 min to 3 h after acquisition to sustain late odor memory (12). The two distinct components of late odor memory, ASM and ARM (16), differ in both temporal dynamics and molecular mechanisms. Whereas ARM requires the active zone protein bruchpilot (40), ASM is not only tomosyn-dependent, according to our observations, but also requires synapsin, a conserved PKA phosphorylation target associated with synaptic vesicles (1). Adult *synapsin* mutant flies exhibit impaired ASM in aversive odor learning. Furthermore, PKA-dependent phosphorylation of synapsin within Kenyon cells is necessary to support larval appetitive odor learning (41, 42). Thus, both tomosyn and synapsin are required for the cAMP-dependent ASM phase of associate learning.

How might synapsin and tomosyn function together in ASM? Mechanistically, PKA phosphorylation of synapsin is implicated in the mobilization and supply of synaptic vesicles from the reserve pool to the active zone (12, 43, 44), whereas PKA phosphorylation of tomosyn promotes SNARE complex assembly (10). This suggests that enhanced vesicle delivery and increased priming capacity through PKA regulation of synapsin and tomosyn, respectively, may act in concert to maintain synaptic strength in support of ASM. Because knockdown of either protein disrupts ASM, it seems that both vesicle mobilization and enhanced priming capacity are required for this phase of synaptic plasticity.

cAMP-Dependent Regulation of Tomosyn Represents a Potential Mechanism for the Synaptic Plasticity Supporting Late ASM. Several lines of evidence suggest that PKA-dependent modulation of tomosyn function provides a possible molecular mechanism for the transduction of cAMP signaling into synaptic plasticity within the olfactory system underlying ASM. First, at the level of the NMJ, we have shown that tomosyn regulates synaptic strength and that this regulation occludes cAMP-dependent synaptic enhancement. Second, within the olfactory neuronal network, we have demonstrated that tomosyn function is likely required within Kenyon cells to support ASM: the cells that receive instructive signals to initiate cAMP-dependent synaptic changes underlying appropriate behavioral plasticity (33, 34, 45). Third, synaptic output from Kenyon cells is necessary to support both early and late odor memories (35, 46, 47). Fourth, DPM signaling onto Kenyon cells is required for late aversive odor memory, and DPM neurons stain positive for the amnesiac peptide (36), which is known to stimulate cAMP production (38, 39). Fifth, enhanced synaptic transmission in cultured neurons induced by the vertebrate amnesiac homolog PACAP requires PKA-dependent tomosyn phosphorylation (10). Sixth, postacquisitional PKA activity is necessary for late aversive odor memory (12) and is likely mediated by an A kinase-anchoring protein (AKAP)-bound pool of PKA holoenzymes within Kenyon cells (14). Finally, biochemical evidence demonstrating that PKA-dependent phosphorylation of tomosyn reduces its affinity for the SNARE machinery suggests a potential mechanistic link between cAMP signaling within Kenyon cells and the up-regulation of synaptic strength (7, 10).

On the basis of this evidence, we postulate that loss of tomosyn inhibitory function leads to a generalized up-regulation of synaptic strength at *Drosophila* synapses. In Kenyon cells enhanced synaptic transmission resulting from loss of tomosyn likely occludes cAMP-dependent plasticity. This speculation is supported by the observed occlusion of forskolin-dependent synaptic enhancement at the NMJ after *tomosyn* RNAi. Similarly, PACAP-induced synaptic plasticity in cultured neurons is occluded when tomosyn is no longer phosphorylatable by PKA (10). We further speculate that within Kenyon cells the phosphorylation of *Drosophila* tomosyn is due to postacquisitional, DMP-induced PKA activity. This hypothesis would fit with the observed requirement of AKAP-bound PKA for late but not early ASM (14). It is thus tempting to speculate that tomosyn phosphorylation is dependent on localized signaling via AKAPs at specific subdomains of Kenyon cells that occur after early ASM is established.

Materials and Methods

Electrophysiology. Two-electrode voltage clamp was performed as previously described (48). Briefly, ventral longitudinal muscles 6 and 7 in abdominal segments 3–4 of third-instar larvae were clamped at −60 mV using an MDS Analytical Technologies GeneClamp 500B amplifier, in standard *Drosophila* saline (135 mM NaCl, 5 mM KCl, 4 mM MgCl2, 1.8 mM $CaCl_2$, 5 mM TES, and 72 mM sucrose). Electrodes (resistance 10–20 MΩ) were filled with 3 M KCl. Segmental nerves innervating muscles 6 and 7 were stimulated using a Grass S48 stimulator via a suction electrode filled with bath saline. All electrophysiological recordings were digitized and analyzed using a Digidata 1322A digitizer (Axon Instruments) with PClamp 10 software. Statistical significance was determined using unpaired Student *t* tests (for normally distributed data) or nonparametric Mann-Whitney tests (when post hoc *F* tests determined that variances were significantly different). Asterisks in figures indicate statistical significance: $***P < 0.0001$, $**P < 0.001$, $*P < 0.05$.

Immunohistochemistry. NMJs of muscles 6 and 7 of third-instar larvae were labeled with affinity-purified tomosyn antibodies (final dilution 1:2,000) raised in rabbits against a synthetic peptide comprising amino acids 25–44 of *Drosophila* tomosyn (EQEIQEQLKADHFTLKKTFR). FITC- and TRITC-conjugated goat anti-rabbit secondary antibodies (1:500 dilution) were obtained from Jackson Immunoresearch Laboratories. Fluorescently conjugated anti-HRP (Jackson Immunoresearch Laboratories) was used at 1:200. Confocal images were captured using an Olympus Fluoview FV500 laser scanning confocal system. Quantification of staining intensity was performed as previously described (49).

Quantitative RT-PCR. Total mRNA was isolated from adult flies using TRIzol (Invitrogen) extraction. Genomic DNA was removed by TURBO-DNAFree Kit (Ambion). Reverse transcription was done from 1 μg of purified mRNA using the SuperScript III First-Strand Synthesis System (Invitrogen) with oligo(dT) primers. RT-PCR was performed using fluorescent detection and quantitation of SYBR green-labeled PCR product using an MJResearch Opticon2 real-time thermocycler. The cycle threshold [C(t)] value for tomosyn was normalized to that of an actin 5C control using the equation: $\Delta C(t)\text{sample} = C(t)\text{tomosyn} - C(t)\text{actin 5C}$. Normalized C(t) values for *tomosyn* RNAi samples were then referenced to the wild type (calibrator) to determine the relative amount of tomosyn mRNA using the equation: $\Delta\Delta C(t)\text{sample} = \Delta C(t)\text{sample} - \Delta C(t)\text{calibrator}$.

Behavioral Experiments. Flies were raised at 28 °C and 60% relative humidity with a 14:10 h light/dark cycle on cornmeal-based food (50). Flies to be tested in behavioral experiments were F1 progeny of homozygous parental crosses. Behavioral experiments were performed in dim red light at 70% relative humidity with isoamyl acetate (1/3 dilution in mineral oil) and ethylacetate (1/5 dilution in mineral oil) used as olfactory cues and 120-V AC pulses (1.3-s pulse duration, with 12 pulses applied during 1 min of training) as the unconditioned stimulus for the associative experiments, as previously described (14, 46). Flies were tested for odor memories 3 min or 3 h after the training session to obtain performance of early or late memory. Statistical analysis was done using one-way ANOVA with a post hoc test including the least significant difference correction for multiple comparisons.

ACKNOWLEDGMENTS. This research was funded by National Institutes of Health Grant RO1 MH073156 (to J.E.R.), Deutsche Forschungsgemeinschaft Grant SCHW1410/1-1 (to M.S.), and Free University Berlin Grant 02370 (to M.S.). Essential reagents and services were provided by the Bloomington Stock Center and the University of Illinois at Chicago's Research Resource Center.

1. Sudhof TC (2004) The synaptic vesicle cycle. *Annu Rev Neurosci* 27:509–547.
2. Sutton RB, Fasshauer D, Jahn R, Brunger AT (1998) Crystal structure of a SNARE complex involved in synaptic exocytosis at 2.4 A resolution. *Nature* 395:347–353.
3. Hammarlund M, Palfreyman MT, Watanabe S, Olsen S, Jorgensen EM (2007) Open syntaxin docks synaptic vesicles. *PLoS Biol* 5:e198.
4. Fujita Y, et al. (1998) Tomosyn: A syntaxin-1-binding protein that forms a novel complex in the neurotransmitter release process. *Neuron* 20:905–915.
5. Hatsuzawa K, Lang T, Fasshauer D, Bruns D, Jahn R (2003) The R-SNARE motif of tomosyn forms SNARE core complexes with syntaxin 1 and SNAP-25 and down-regulates exocytosis. *J Biol Chem* 278:31159–31166.
6. Pobbati AV, Razeto A, Böddener M, Becker S, Fasshauer D (2004) Structural basis for the inhibitory role of tomosyn in exocytosis. *J Biol Chem* 279:47192–47200.
7. Sakisaka T, et al. (2008) Dual inhibition of SNARE complex formation by tomosyn ensures controlled neurotransmitter release. *J Cell Biol* 183:323–337.
8. Yamamoto Y, et al. (2010) Tomosyn inhibits synaptotagmin-1-mediated step of Ca2+-dependent neurotransmitter release through its N-terminal WD40 repeats. *J Biol Chem* 285:40943–40955.
9. Sakisaka T, et al. (2004) Regulation of SNAREs by tomosyn and ROCK: Implication in extension and retraction of neurites. *J Cell Biol* 166:17–25.
10. Baba T, Sakisaka T, Mochida S, Takai Y (2005) PKA-catalyzed phosphorylation of tomosyn and its implication in Ca2+-dependent exocytosis of neurotransmitter. *J Cell Biol* 170:1113–1125.
11. Gladycheva SE, et al. (2007) Receptor-mediated regulation of tomosyn-syntaxin 1A interactions in bovine adrenal chromaffin cells. *J Biol Chem* 282:22887–22899.
12. Li W, Tully T, Kalderon D (1996) Effects of a conditional *Drosophila* PKA mutant on olfactory learning and memory. *Learn Mem* 2:320–333.
13. Skoulakis EM, Kalderon D, Davis RL (1993) Preferential expression in mushroom bodies of the catalytic subunit of protein kinase A and its role in learning and memory. *Neuron* 11:197–208.
14. Schwaerzel M, Jaeckel A, Mueller U (2007) Signaling at A-kinase anchoring proteins organizes anesthesia-sensitive memory in *Drosophila*. *J Neurosci* 27:1229–1233.
15. Kandel ER (2001) The molecular biology of memory storage: A dialogue between genes and synapses. *Science* 294:1030–1038.
16. Quinn WG, Dudai Y (1976) Memory phases in *Drosophila*. *Nature* 262:576–577.
17. Margulies C, Tully T, Dubnau J (2005) Deconstructing memory in *Drosophila*. *Curr Biol* 15:R700–R713.
18. Vosshall LB, Stocker RF (2007) Molecular architecture of smell and taste in *Drosophila*. *Annu Rev Neurosci* 30:505–533.
19. Fiala A, et al. (2002) Genetically expressed cameleon in *Drosophila melanogaster* is used to visualize olfactory information in projection neurons. *Curr Biol* 12:1877–1884.
20. Wang JW, Wong AM, Flores J, Vosshall LB, Axel R (2003) Two-photon calcium imaging reveals an odor-evoked map of activity in the fly brain. *Cell* 112:271–282.
21. Shang Y, Claridge-Chang A, Sjulson L, Pypaert M, Miesenböck G (2007) Excitatory local circuits and their implications for olfactory processing in the fly antennal lobe. *Cell* 128:601–612.
22. Gracheva EO, et al. (2006) Tomosyn inhibits synaptic vesicle priming in Caenorhabditis elegans. *PLoS Biol* 4:e261.
23. McEwen JM, Madison JM, Dybbs M, Kaplan JM (2006) Antagonistic regulation of synaptic vesicle priming by Tomosyn and UNC-13. *Neuron* 51:303–315.
24. Weimer RM, et al. (2006) UNC-13 and UNC-10/rim localize synaptic vesicles to specific membrane domains. *J Neurosci* 26:8040–8047.
25. Siksou L, et al. (2009) A common molecular basis for membrane docking and functional priming of synaptic vesicles. *Eur J Neurosci* 30:49–56.
26. Gracheva EO, Maryon EB, Berthelot-Grosjean M, Richmond JE (2010) Differential regulation of synaptic vesicle tethering and docking by UNC-18 and TOM-1. *Front Synaptic Neurosci* 2:141.
27. Gracheva EO, Hadwiger G, Nonet ML, Richmond JE (2008) Direct interactions between C. elegans RAB-3 and Rim provide a mechanism to target vesicles to the presynaptic density. *Neurosci Lett* 444:137–142.
28. Schwärzel M, Müller U (2006) Dynamic memory networks: Dissecting molecular mechanisms underlying associative memory in the temporal domain. *Cell Mol Life Sci* 63:989–998.
29. Heisenberg M (2003) Mushroom body memoir: From maps to models. *Nat Rev Neurosci* 4:266–275.
30. Gerber B, Tanimoto H, Heisenberg M (2004) An engram found? Evaluating the evidence from fruit flies. *Curr Opin Neurobiol* 14:737–744.
31. McGuire SE, Deshazer M, Davis RL (2005) Thirty years of olfactory learning and memory research in *Drosophila melanogaster*. *Prog Neurobiol* 76:328–347.
32. Keene AC, Waddell S (2007) *Drosophila* olfactory memory: Single genes to complex neural circuits. *Nat Rev Neurosci* 8:341–354.
33. Zars T, Fischer M, Schulz R, Heisenberg M (2000) Localization of a short-term memory in *Drosophila*. *Science* 288:672–675.
34. Gervasi N, Tchénio P, Preat T (2010) PKA dynamics in a *Drosophila* learning center: Coincidence detection by rutabaga adenylyl cyclase and spatial regulation by dunce phosphodiesterase. *Neuron* 65:516–529.
35. McGuire SE, Le PT, Davis RL (2001) The role of *Drosophila* mushroom body signaling in olfactory memory. *Science* 293:1330–1333.
36. Waddell S, Armstrong JD, Kitamoto T, Kaiser K, Quinn WG (2000) The amnesiac gene product is expressed in two neurons in the *Drosophila* brain that are critical for memory. *Cell* 103:805–813.
37. Quinn WG, Sziber PP, Booker R (1979) The *Drosophila* memory mutant amnesiac. *Nature* 277:212–214.
38. Feany MB, Quinn WG (1995) A neuropeptide gene defined by the *Drosophila* memory mutant amnesiac. *Science* 268:869–873.
39. Moore MS, et al. (1998) Ethanol intoxication in *Drosophila*: Genetic and pharmacological evidence for regulation by the cAMP signaling pathway. *Cell* 93:997–1007.
40. Knapek S, Sigrist S, Tanimoto H (2011) Bruchpilot, a synaptic active zone protein for anesthesia-resistant memory. *J Neurosci* 31:3453–3458.
41. Knapek S, Gerber B, Tanimoto H (2010) Synapsin is selectively required for anesthesia-sensitive memory. *Learn Mem* 17:76–79.
42. Michels B, et al. (2011) Cellular site and molecular mode of synapsin action in associative learning. *Learn Mem* 18:332–344.
43. Akbergenova Y, Bykhovskaia M (2007) Synapsin maintains the reserve vesicle pool and spatial segregation of the recycling pool in *Drosophila* presynaptic boutons. *Brain Res* 1178:52–64.
44. Akbergenova Y, Bykhovskaia M (2010) Synapsin regulates vesicle organization and activity-dependent recycling at *Drosophila* motor boutons. *Neuroscience* 170:441–452.
45. McGuire SE, Le PT, Osborn AJ, Matsumoto K, Davis RL (2003) Spatiotemporal rescue of memory dysfunction in *Drosophila*. *Science* 302:1765–1768.
46. Schwaerzel M, Heisenberg M, Zars T (2002) Extinction antagonizes olfactory memory at the subcellular level. *Neuron* 35:951–960.
47. Dubnau J, Tully T (2001) Functional anatomy: From molecule to memory. *Curr Biol* 11: R240–R243.
48. Chen K, Merino C, Sigrist SJ, Featherstone DE (2005) The 4.1 protein coracle mediates subunit-selective anchoring of *Drosophila* glutamate receptors to the postsynaptic actin cytoskeleton. *J Neurosci* 25:6667–6675.
49. Chen K, et al. (2010) Neurexin in embryonic *Drosophila* neuromuscular junctions. *PLoS ONE* 5:e11115.
50. Guo A, et al. (1996) Conditioned visual flight orientation in *Drosophila*: dependence on age, practice, and diet. *Learn Mem* 3:49–59.